http://journal.uir.ac.id/index.php/JGEET

E-ISSN : 2541-5794
P-ISSN : 2503-216X

Journal of Geoscience,
Engineering, Environment, and Technology
Vol 10 No 2 2025

RESEARCH ARTICLE

Extraction of Manganese Ore from East Nusa Tenggara-Indonesia for Production of Mn(II)-Terephthalate and Mn(II)-Tartrate Coordination Polymers

Faustina De Yesu Prisila Abi [1,*], Rachmat Triandi Tjahjanto[2], Yuniar Ponco Prananto[2]

[1] *Department of Chemistry, Widya Mandira Catholic University, Kupang, Indonesia*
[2] *Department of Chemistry, Brawijaya University, Malang, Indonesia*

* Corresponding author: faustinadeyesuprisilaabi@unwira.ac.id
Tel.:+62 85-333-419-351
Received: Feb 24, 2035; Accepted: Jun 30, 2025.
DOI: 10.25299/jgeet.2025.10.02.21556

Abstract

Pyrolusite, a manganese ore from East Nusa Tenggara (Indonesia), was explored and utilized in the production of crystalline Mn(II) based coordination polymers materials, namely Mn(II)-terephthalate and Mn(II)-tartrate. The pyrolusite was extracted into Mn(II) sulfate by acid method in the presence of hydrogen peroxide. The Mn(II) sulfate, characterized by X-ray fluorescence (XRF), infrared spectroscopy (IR), and X-ray powder diffraction (PXRD), was then used as a precursor in the production of crystalline Mn(II) based coordination polymers materials using a solution method at room temperature. Two ligands, terephthalate and tartrate, were used separately, in which the terephthalate complex was prepared using a layered solution technique, while the tartrate complex was made using a direct mixing technique. The synthesized Mn(II) coordination polymers were then characterized by FTIR and PXRD. This study finds that the manganese ore was extracted as $MnSO_4$ compounds with purity of 96.88% and average crystallite size of 103 nm. The $MnSO_4$ was successfully converted into crystalline Mn(II) coordination polymers materials. Based on IR and PXRD analyses, the crystalline products were identified as Mn(II)-aqua-terephthalato and Mn(II)-aqua-tartrato hydrate complexes, in which the former complex display 3D networks and the latter complex display 2D sheets of polymeric structures.

Keywords: Ore extraction, Pyrolusite, Coordination polymers, Terephthalate, Tartrate

1. Introduction

Manganese ore is one of the abundant minerals found in Indonesia, for example, *rhodonite,* which is found in Anabanua Village, South Sulawesi (Bakri et al., 2024), rhodoxite in Baolemo red limestone (Yusuf et al., 2023) and pyrolusite, which is found in the East Nusa Tenggara (ENT) (Abi et al., 2023). Manganese in the ENT Province, particularly in the Luniup village, is massively reserved, but it has not been optimally explored due to several considerations. However, local communities have been exploring it, but mostly by directly selling small size ore pieces to collectors at a very low rate, around Rp.1,200/kg on the local market (Supriadi et al., 2017).

Several research reported that the pyrolusite can be converted into manganese oxide, both MnO_2 and Mn_3O_4, from nano to micro sizes and in a variety of morphologies (Abi et al., 2019; Kusumaningrum et al., 2020). Conversion of the ore into their oxides can be explored to diversify the ore derivatives, as well as to increase the economic value of the ores. The manganese oxide can be further used in biomedicine or used as semiconductors, supercapacitors, adsorbents, sensors, catalysts, etc (Dawadi et al., 2020; Paulose and Mohan, 2019). The economic value of the manganese ore can also be increase by using the extracted mineral, not only in their oxide form but also in their other compound, such as $MnSO_4$, to further developed as coordination polymers – based functional materials.

Functional materials based on Mn(II) coordination polymers material, including metal-organic frameworks, and their potential applications have been reported. Mn(II) with 1,3,5-benzenetricarboxylate ligand was successfully used for toluene adsorption (Zhang et al., 2022). Mn(II) with 2,5-dihydroxyterephthalate ligand performs high BPA degradation when combined with CNT-hemin (Hou et al., 2022). Mn(II) with 2,6-naphthalenedicarboxylate ligand was used as a versatile photo-sensitizer for light energy conversion, molecular electronics or photonic devices (Dawood et al., 2021). Mn(II)-tetratopic-phosphonate as a pediatric reference range for usage in clinical settings against sepsis illness was also developed, which can selectively, sensitively, and swiftly detect arginine in pure aqueous solutions or biofluids like human urine and bovine serum, which would be extremely beneficial (Chakraborty et al., 2022). Those Mn(II) coordination polymers were made using different types of ligands and in variety of synthetic methods.

In this work, terephthalate ($C_8H_4O_4^{-2}$) and tartrate ($C_4H_4O_6^{-2}$) ligands were employed separately to produce Mn(II) coordination polymers from the extracted pyrolusite. These ligands were reported to be used in the construction of a 3D polymeric network in the presence of transition metal ions. Some of their metal complexes show large surface areas and homogenous porosity. These ligands have also been extensively utilized in the synthesis of many transition metal complexes (Jagtap et al., 2022; Li et al., 2010; Yang et al., 2020; Zhao et al., 2022). Mn(II)-terephthalate and its derivatives were used for a variety of applications, including removing volatile organic compounds (Chen et al., 2022), catalysing chemical

reactions (Yadav et al., 2020), and absorbing H_2 and CO_2 gasses (Asghar et al., 2021). Meanwhile, Mn(II)-tartrate and its derivatives, have been utilized for non-linear optics (Gandhimathi et al., 2015), therapeutic agent (Chakraborty et al., 2021), and catalyst in asymmetric epoxidation (Jia et al., 2020).

Specifically, $MnSO_4$ as the manganese source used in this work was originated from the leaching product of pyrolusite from the Luniup village in the ENT Indonesia. The ore must be leached first into $MnSO_4$ because there is other Mn species found in the pyrolusite, such as Mn(IV), which have different chemical properties and may initiate further reaction and alter the synthesis of the Mn(II)-terephthalate and Mn(II)-tartrate. The leaching process was carried out under acidic conditions in the presence of H_2O_2 as a reducing agent. In this condition, Mn(IV) was reduced into Mn(II). This leaching method was selected due to its effectiveness (Li et al., 2017; Sandag-Ochir et al., 2021). In addition, the $MnSO_4$ was chosen since the Mn(II) precursor should be easy to dissolve in aqueous solvent, a crucial factor in the crystallization of Mn(II) coordination polymers from green solvent of H_2O. According to the CRC Handbook of Chemistry and Physics, $MnSO_4$ is very soluble in water with a solubility of 63.7 g per 100 g of H_2O at 25 ^{0}C (Lide, 2010).

Crystallization of Mn(II) coordination polymers using terephthalate or tartrate ligands reported in this paper is developed from previous work but using different manganese precursor. To the best of our knowledge, synthesis of Mn(II)-terephthalate and Mn(II)-tartrate compounds from manganese ore particularly via $MnSO_4$ route has never been reported. Previously, lab-grade Mn(II) salt was used as the precursor. The Mn(II)-terephthalate could be synthesized by solvothermal (Sundriyal et al., 2019b), microwave (Abd El Salam and Zaki, 2019), and sonication (Asghar et al., 2020) methods, whereas the Mn(II)-tartrate can be prepared by gel (Gandhimathi et al., 2015; Jagtap et al., 2022), solution (Khunur and Prananto, 2018), and reactive crystallization (Saravanabharathi and Murugavel, 2021) methods.

The variety of synthetic method in the production of Mn(II) coordination polymers also widens the possibility of converting the manganese ore into the targeted Mn(II) coordination polymers. Apart from many synthetic methods, a layered solution technique was chosen in the crystallization of Mn(II)-terephthalate compound, while a direct mixing technique was used for the crystallization of Mn(II)-tartrate compound. These techniques are simple and easy (all in one pot vessel and require simple apparatus), environmentally friendly (performed at ambient temperature and use greener solvent *i.e.* water and/or methanol), and the products can be easily isolated (easy to separate by paper filtration).

2. Methods and Materials

2.1 Chemicals and instrumentation

Chemicals and materials used in this study were manganese ore from Luniup Village, East Nusa Tenggara (Indonesia), sulphuric acid (Merck), ammonium hydroxide (Merck), hydrogen peroxide (Merck), terephthalic acid (Sigma-Aldrich), potassium sodium tartrate hydrate (Dian Lab), and methanol (Merck).

Chemical instrumentations for characterization of the products used in this study were infrared spectroscopy (IRSpirit Shimadzu), powder X-ray diffraction (PANalytical X'Pert3 Powder-XRD), and X-ray fluorescence (PANalytical Minipal 4 X-Ray Fluorescence). The infrared spectroscopy (IR) and powder X-ray diffraction (PXRD) analyses were conducted at Brawijaya University, Indonesia, whereas the X-ray fluorescence (XRF) was performed at the State University of Malang, Indonesia

2.2 Extraction of pyrolusite into $MnSO_4$

Production of $MnSO_4$ from the ore was carried out using an identical method as reported previously (Abi et al., 2023). A total of 10 grams of ore powder were added to 50 mL of 4M H_2SO_4. The mixture was stirred for 30 minutes at room temperature. The mixture was then added with 25 mL of 2M H_2O_2 and kept stirred for another 1.5 hours (total leaching time was two hours). The mixture was then filtered off using Whatman filter paper no 41, in which a clear reddish-purple solution was obtained. The filtrate was then added with 25% NH_4OH dropwise until the pH of the solution reached 7. Brown precipitate was yielded by allowing the solution to stand at room temperature overnight. The precipitate was then separated by Whatman filter paper no 41, resulting in a clear solution. A white crystalline solid was produced after slow evaporation of the solution. The solid was then dried and saved in a desiccator for a few days using silica gel beads as a drying agent.

The resulting in $MnSO_4$ was then characterized and used as a precursor in the syntheses of Mn(II)-terephthalate and Mn(II)-tartrate coordination polymers. The $MnSO_4$ was characterized by X-Ray Fluorescence (20 kV/45μA; 60 second) for elemental composition, infrared spectroscopy (ATR, 4000-400 cm^{-1}) for functional group identification, and powder X-Ray diffraction (2θ = 5°-70°, Cu-Kα λ = 1.54187 Å) for compound determination by comparing the powder diffraction patterns with that of identical compound from the Crystallography Open Database (COD), and for average crystallite size measurement based on Scherrer equation using XRD Crystallite (grain) Size Calculator (Insta Nano, 2025).

2.3 Synthesis Mn(II) with terephtalate ligand

A total of 100 mg of $MnSO_4$ was dissolved in 10 mL of distilled water. Then, the solution was placed in a test tube. Next, 5 mL of water-methanol (1:1) solution was slowly added on top of the metal solution. For the top layer, 110 mg of terephthalic acid was added with 5 mL of methanol and four drops of 25% NH_4OH, and then added with 1 mL of distilled water was added and added above the water-methanol solution. After that, the reaction was allowed to stand at room temperature for one month. The solid product that formed was isolated, washed with distilled water, and then dried at 100 ^{0}C for an hour.

2.4 Synthesis Mn(II) with tartrate ligand

A 453 mg of $MnSO_4$ was first dissolved in 10 mL of distilled water. Next, it was mixed and stirred with KNa-tartrate solution (847 mg; 40 mL) for two hours. After that, the solution was allowed to stand and slowly evaporated at room temperature, in which colourless crystals started forming. After three months, the crystals were isolated, washed with distilled water, and then saved in a desiccator equipped with silica gel beads for several days.

2.5 Characterization of Mn(II) coordination polymers

The synthesized Mn(II) coordination polymers were characterized by powder X-Ray diffraction (2θ = of 5°-70°, Cu-Kα λ = 1.54187 Å) and infrared spectroscopy (ATR, 4000-400 cm^{-1}). Crystal structures of the synthesized

Mn(II) coordination polymers were generated by comparing their powder diffraction patterns with reported compounds in the Crystallography Open Database (COD). Diffraction profile fitting and phase identification were conducted using PANalytical HighScore software ver. 3.0e (3.0.5). Graphical structures of the compound are generated using Olex2. Ver. 1.2.10 (Dolomanov et al., 2009).

3. Results and Discussion

3.1 Extraction of pyrolusite

From 10 gram of pyrolusite, 17.48 grams of white powdery $MnSO_4$ (Fig. 1) were obtained with a purity of 96.88%, based on XRF analysis (Table 1). The percentages of MnO and Mn in the $MnSO_4$ sample were 30.08% and 50.27%, respectively. This result is higher than that of earlier research, which reported that the purity of $MnSO_4$ was only 79.11% with a percentage of MnO of 27.56% (Sumardi et al., 2013).

Fig. 1. Physical appearance of the $MnSO_4$

Table 1. XRF analysis of the extracted $MnSO_4$

Compound	Percentage (%)	Element	Percentage (%)
MnO	30.08	Mn	50.27
SO_3	66.8	S	45.1
CaO	0.62	Ca	0.85
CuO	0.16	Cu	0.3
MoO_3	2	Mo	3
Yb_2O_3	0.08	Yb	0.2
Re_2O_7	0.1	Re	0.2

The presence of $MnSO_4$ was also confirmed by infrared spectroscopy and powder XRD analyses. Infrared spectra of the extraction product (Fig. 2) exhibit an intense sharp peak at 1402 and an intense but wider band around 1127 cm^{-1}, which correspond to the NH_4^+ bending mode and sulfur-oxygen stretching mode of sulfate, respectively. The presence of sulfate group is also confirmed by the symmetrical vibration of the anion at 981 cm^{-1} and by the out-of-plane bending vibration around 650-600 cm^{-1}. A broadband around 3200 cm^{-1} suggests the presence of O–H, which in this study, may overlap with the characteristic bands of the amide group from the NH_4^+ (Guo et al., 2010; Kusumaningrum et al., 2018; Nakamoto, 2006; Nyquist and Kagel, 1971; OChemOnline, 2011; Sagar et al., 2021; Sagunthala et al., 2013).

Moreover, powder-XRD analysis indicates that the product is a multiphase of $MnSO_4$ compounds, based on COD ID no. 9014164, 9012360, 7218173, namely $MnSO_4{\cdot}4H_2O$, $MnSO_4{\cdot}5H_2O$, and $[NH_4]_8[Mn_8(SO_4)_{12}]$, respectively (Fig. 3). This is supported by the high-intensity peaks found at 2-theta angles of 27.72°, 29.32°, and 29.86° for $MnSO_4{\cdot}4H_2O$; and at 17.02°, 20.50°, and 32.90° for $MnSO_4{\cdot}5H_2O$. The 2-theta angle of 15.12° is predicted to correspond to the peak of the $[NH_4]_8[Mn_8(SO_4)_{12}]$ (Anderson et al., 2012; Behera et al., 2014; Caminiti et al., 1982). The presence of ammonium is also indicated by the IR analysis, as described above. All three $MnSO_4$ compounds form identical morphology and color, the composition (%) of each compound within the mixture was unidentifiable. In addition, based on the top 25 peaks of the diffraction peaks, the average crystallite size of the $MnSO_4$ is around 103 nm. The multiphase $MnSO_4$ was then used as for the next stage without further purification due to only the Mn(II) ions from the $MnSO_4$ precursors considered to be needed in the formation of the Mn(II) coordination polymers.

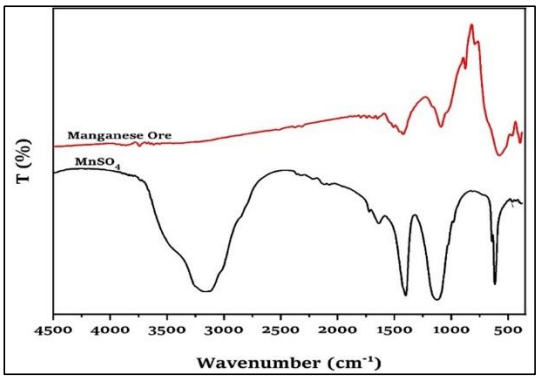

Fig. 2. Infrared spectra of pyrolusite (top) and the extracted $MnSO_4$ (bottom).

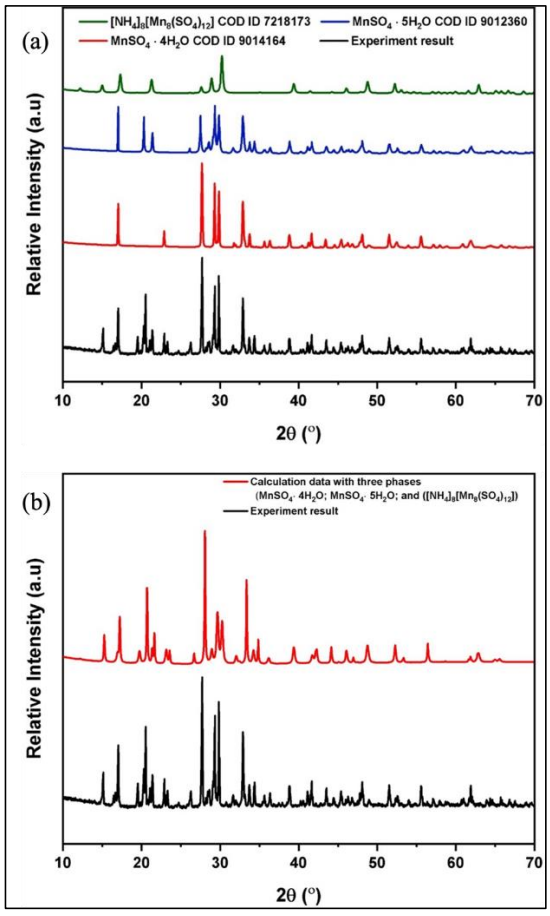

Fig. 3. Powder diffraction pattern of the obtained $MnSO_4$ compared to each reference compounds (top) and compared to combined reference compounds (bottom).

3.2 Synthesis and Characterization of Mn(II) with terephthalate ligand

Coordination polymer of Mn(II) with terephthalate ligand was prepared by a layered solution technique, as adopted from the previous report (Prananto et al., 2022), except that aqueous NH_4OH was added into the methanolic solution to fully dissolve the terephthalic acid. After several days, the three layers of solution were merged into a clear homogenous solution. White flower-like crystals were formed (Fig. 4), in which 28.13 mg of crystals were obtained from 100 mg of $MnSO_4$ used. The lack of product yield is predicted due to the low concentration of the precursors and ligand used in this work (Czaja et al., 2009; Elazar, 2022; Lee et al., 2013; Ma et al., 2023; Santos and Luz, 2020; Stock and Biswas, 2012; Zheng et al., 2023). However, the crystals produced in this study are much bigger than that of from previous studies (Sundriyal et al., 2019a) in which in previous report, the precipitation was isolated using centrifugation, which indicates that the synthesis product was in fine powder. The crystals obtained were then characterized by infrared spectroscopy and powder XRD to confirm the formation of Mn(II)-terephthalate.

Fig. 4. Synthesized Mn(II) with terephthalate ligand

Infrared spectra (Fig. 5) of the synthesized Mn(II)-terephthalate display a broad absorption band associated with the vibration of the –OH group of water molecules around 3400 cm^{-1}. The presence of asymmetric and symmetric stretching vibrations of the carboxylate group is observed at 1546.01 and 1386.28 cm^{-1}. Coordination bond between the Mn(II) and the terephthalate ligand is indicated from the absorption band at 751.51 cm^{-1} (Hu et al., 2016; Sundriyal et al., 2019a). Thus, the synthesized compound is confirmed to have coordinated terephthalates.

Table 2. Crystallography data of Mn(II)-terephthalate

Parameters	Mn(II)-terephthalate	
	COD ID 2103339	This work(*)
Crystal system	Monoclinic	Monoclinic
Space group	*C*2/c	*C*2/c
a	18.7213(13)	18.81(3)
b	6.590(4)	6.560(8)
c	7.4035(6)	7.373(6)
α	90	90
β	99.287(3)	99.58(6)
γ	90	90

(*) calculated based on powder XRD data using HighScore software

Meanwhile, the powder XRD diffraction profile (Fig. 5) of the synthesized compound shows the five highest peaks located at 2θ angles of 9.64°; 14.55°; 18.6°; 30.4°; and 34.02°. The diffraction profile of the synthesized compound is nearly identical to that of a known compound of Mn(II)-terephthalate dihydrate or reported as COD 2103339 (Hu et al., 2016; Kaduk, 2002; Sundriyal et al., 2019a), in which the complex was crystallized in the monoclinic crystal system with space group of *C*2/c. Calculation of unit cell parameters by HighScore software is also in agreement with the Mn(II)-terephthalate dihydrate (Table 2).

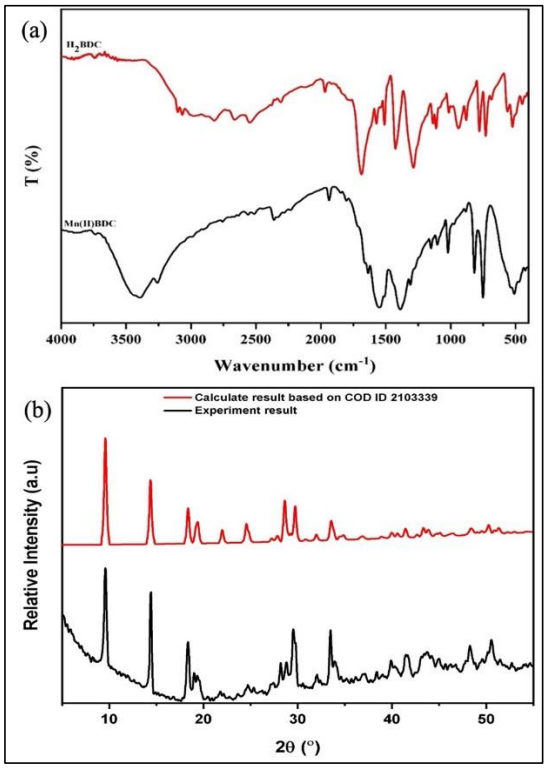

Fig. 5. Infrared spectra (a) and powder diffraction pattern (b) of the Mn(II) complex with terephthalate ligand

3.3 Synthesis and Characterization of Mn(II) with tartrate ligand

Coordination polymers of Mn(II) with tartrate ligand, also known were prepared by directly mixing metal and ligand solution and stirred at 50-60 ºC for two hours. The crystals were formed upon the slow evaporation of the mother liquor at room temperature. After isolating and drying the crystal, white-ish crystalline powder was obtained (Fig. 6), in which 113.7 mg of product was yielded from 453 mg of $MnSO_4$ used. The small amount of product obtained can be caused by the low concentration of metal ion and ligand, as well as due to short stirring time (Czaja et al., 2009; Elazar, 2022; Lee et al., 2013; Ma et al., 2023; Santos and Luz, 2020; Stock and Biswas, 2012; Zheng et al., 2023). The crystals obtained were then characterized by FTIR and powder XRD to confirm the formation of Mn(II)-tartrate.

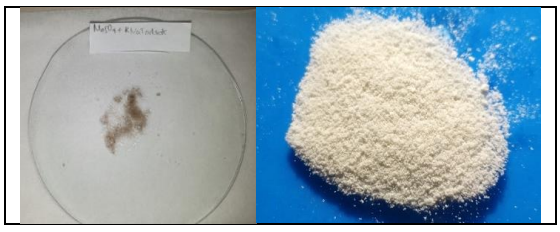

Fig. 6. Synthesis results of Mn(II) with tartrate ligand: products from one reaction vial after separated from the solution (left) and after air dried and grinded (right)

Infrared spectra (Fig. 7) of the synthesized compound display sharp absorptions at 1614.47 and 1567.41 cm^{-1} that indicate the C=O stretching vibrations. A C-H (alkane) bending was observed at 1386.28 cm^{-1}. Meanwhile, the

1322.10 and 1293.57 cm^{-1} peaks, corresponding to the presence of asymmetric C-OH, were also observed. The presence of symmetric C-OH was confirmed by the 1130.90 and 1063.38 cm^{-1} peaks. Meanwhile, absorptions at 626, 561.93, 487.76, and 443.55 cm^{-1} indicate the possible bonds between Mn(II) and the oxygen of the hydroxyl and carboxylate groups (Jagtap et al., 2022; Jethva and Joshi, 2014; Prananto et al., 2022). The peak's shift and different profile around 700-400 cm^{-1} also indicate that there has been a replacement of K^+ and Na^+ ions by Mn^{2+}, which also indicates that there is bond formation between the Mn(II) and oxygen of the tartrate ligands.

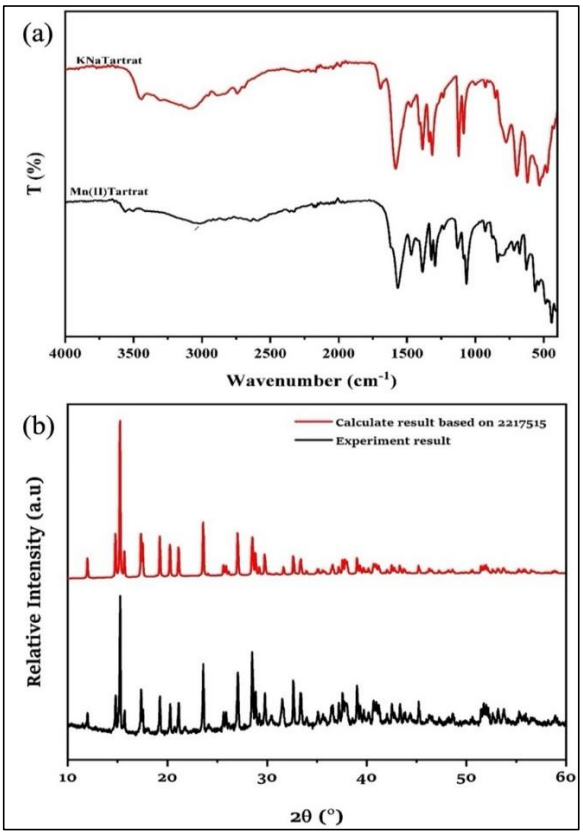

Fig. 7. Infrared spectra (a) and powder diffraction pattern (b) of the synthesized Mn(II) complex with tartrate ligand

Furthermore, powder XRD analysis suggests that the diffraction profile of the synthesized compound is nearly identical to that of known compound Mn(II)-tartrate hydrates with COD no. 2217515 (Ge et al., 2008), in which the complex was crystallized in the monoclinic crystal system with space group of *C*2/c. Calculation of unit cell parameters by HighScore software is also in agreement with the known compound above (Table 3). Therefore, the synthesized compound is confirmed to be Mn(II)-tartrate hydrate.

Table 3. Crystallography data of Mn(II)-tartrate

Parameters	Mn(II)-tartrate	
	COD ID 2217515	This work(*)
Crystal system	Monoclinic	Monoclinic
Space group	*P*2/c	*P*2/c
a	11.029(3)	11.044(1)
b	7.3925(18)	7.390(1)
c	10.165(3)	10.166(2)
α	90	90
β	112.149(3)	112.173(6)
γ	90	90

(*) calculated based on powder XRD data using HighScore software

3.4 Crystal structures of the synthesized Mn(II) coordination polymers

As shwon in Fig. 5, Fig. 7, Tables 2, and Table 3; the synthesized complexes have identical diffraction patterns to that of known compounds in the COD. Therefore, the structure of the synthesized Mn(II) coordination polyemrs can be deduced from the correspond compounds, namely the $[Mn(C_8H_4O_4)(H_2O)_2]_n$ or Mn(II)-aqua-terephthalato (COD ID. 2103339) reported by Kaduk (2002) and the $\{[Mn(C_4H_4O_6)(H_2O)]\cdot H_2O\}_n$ or Mn(II)-aqua-tartrato hydrate (COD ID. 2217515) reported by Ge *et al*. (2008). Crystal structures of those complexes, which illustrate the coordination environment around the metal center and its corresponding crystal packing, are shown in Fig. 8, Fig. 9, and Fig. 10.

In the $[Mn(C_8H_4O_4)(H_2O)_2]_n$ (COD ID. 2103339), the Mn(II) center forms octahedral geometry, in which the Mn center is surrounded by two oxygen atoms from two water ligands (Mn–O = 2.195(4) Å) in a *trans*-position and by four oxygen atoms of the carboxylate groups (Mn–O = 2.189(5) – 2.197(5) Å) from four different terephthalate ligands (Fig. 8).

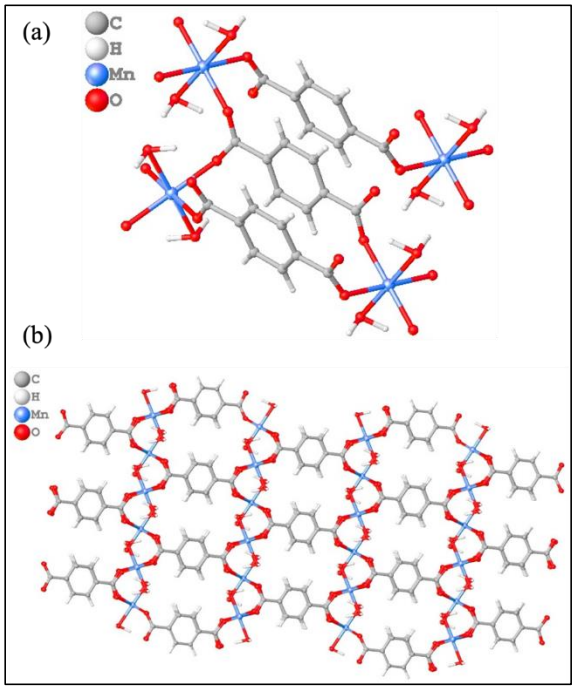

Fig. 8. Coordination environment around the Mn(II) centre (a) and crystal packing of the Mn(II)-terephthalate complex or $[Mn(C_8H_4O_4)(H_2O)_2]_n$ based on COD ID. 2103339 (b)

Moreover, each terephthalate ligand is coordinated to four neighboring Mn(II) centers via one of the carboxylate's oxygen each, resulting in two types of Mn-to-Mn bridging motifs, namely through the whole terephthalate ligand and via the carboxylate (–COO) group of the terephthalate only, with Mn to Mn distances of 9.494 and 4.958 Å, respectively. As a result, the crystal packing of the complex displays 3D network polymeric structure with porosity (Fig. 9). In addition, two types of hydrogen bonds are also observed in the crystal packing involving water ligands and the closest oxygen from one of the carboxylate group with DH···A distances of 2.2–2.4 Å.

Meanwhile, in the $\{[Mn(C_4H_4O_6)(H_2O)]\cdot H_2O\}_n$ (COD ID. 2217515), the Mn(II) center displays a distorted octahedral geometry, in which the Mn center is surrounded by one oxygen atom from water ligand (Mn–O = 2.2018(16) Å) and

by five oxygen atoms from three different tartrate ligands (Mn–O = 2.1036(15) – 2.2518(14) Å) (Fig. 10). Each Mn(II) center is connected to five neighboring Mn(II) center via the tartrate ligand.

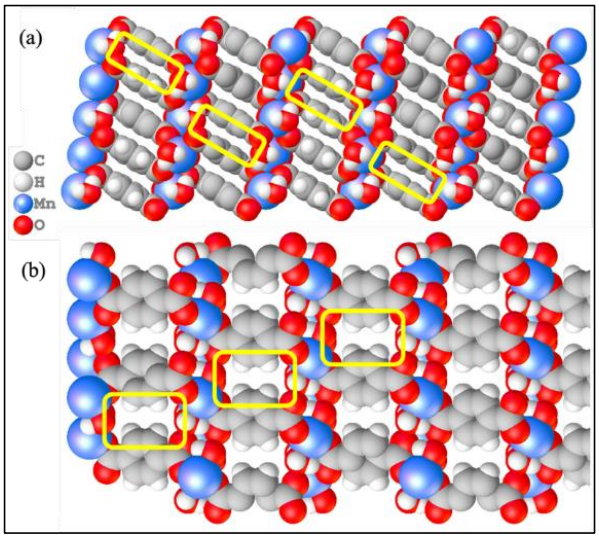

Fig. 9. Part of 3D networks of the Mn(II)-terephthalate complex viewed from two different angles (based on COD ID. 2103339). The voids are highlighted by the yellow square.

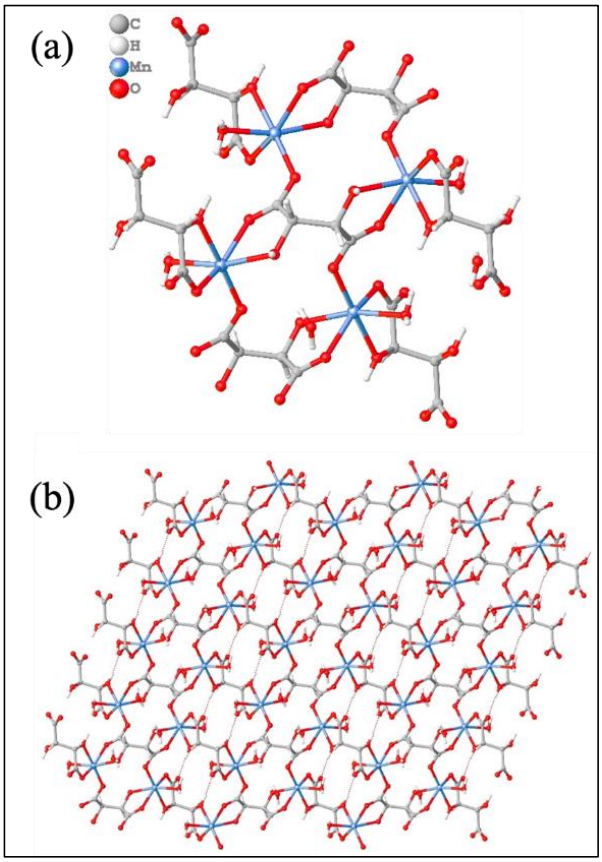

Fig. 10. Coordination environment around the Mn(II) centre (a) and crystal packing of the Mn(II)-tartrate complex or $\{[Mn(C_4H_4O_6)(H_2O)]\cdot H_2O\}_n$ based on COD ID. 2217515 (b); hydrogen bonds are shown in red dots.

On the other hand, each tartrate ligand is coordinated to four different Mn(II) centers, two of the metal centers are connected in a monodentate mode via carboxylate oxygen atom only, and the other two metal centers are bonded in a bidentate fashion via the two closest hydroxyl and carboxylate oxygen atoms. As a result, the crystal packing of the complex forms 2D-sheet polymeric structure. This structure is different from our previous report (Khunur and Prananto, 2018), which shows that the Mn(II)-tartrate forms 3D networks with porosity. This is reasonable since the complexes were synthesized in different method and used different tartrate precursors.

In addition, there is one water molecule in the lattice observed for each Mn(II) complex. The lattice water molecule is then hydrogen bonded to two neighboring oxygen atoms from the tartrate ligands , with D–H···A distances of 2.25–2.29 Å (Fig. 10).

Overall, this study report that the *pyrolusite* can be extracted into high purity $MnSO_4$ and then converted into Mn(II) coordination polymers, which can be further developed as functional material. The two selected crystalline Mn(II) coordination polymers were successfully produced using a one-pot and simple procedure, including using environmentally friendly solvents. However, the yield obtained from this procedure is low, therefore further attempt is needed to optimize the yield and increase the efficiency of the conversion, for example by increasing the concentration of the Mn(II) and the ligands. In addition, further testing can be carried out such as thermal resistance, band gap energy, surface area, dielectric properties, etc, to confirm its potential application as photocatalyst and waste adsorbent or as a dielectric sensor for gas.

4. Conclusion

Manganese ore of East Nusa Tenggara – Indonesia was successfully utilized as precursors in the synthesis of two Mn(II) coordination polymers. White crystalline powder of Mn(II)-aqua-terephthalato and Mn(II)-aqua-tartrato hydrate were obtained, in which both are known compounds, based on COD ID No. 2103339 and ID 2217515, respectively. The Mn(II)-aqua-terephthalato display 3D porous networks, whereas the Mn(II)-aqua-tartrato hydrate display 2D sheets of polymeric structures. Further investigation is needed to optimize the yield.

Acknowledgments

The authors thank the Brawijaya University (Department of Chemistry) and Widya Mandira Catholic University for any support given. The authors also acknowledge the Integrated Research Laboratory (LRT) of Brawijaya University for crystallography analysis.

References

Abd El Salam, H.M., Zaki, T., 2019. A Novel Microwave Synthesis of Manganese Based MOF for Adsorptive of Cd(II), Pb(II) and Hg(II) Ions from Aqua Medium. Egypt. J. Chem. 62, 1237–1251. https://doi.org/10.21608/ejchem.2019.6524.1550

Abi, F.D.Y.P., Kusumaningrum, R., Widayatno, W.B., Wismogroho, A.S., Noviyanto, A., Rochman, N.T., Amal, M.I., 2019. Synthesis of Nanosize Manganese Oxides from Its Ore using Solvothermal Method. IOP Conf. Ser. Mater. Sci. Eng. 578. https://doi.org/10.1088/1757-899X/578/1/012011

Abi, F.D.Y.P., Tjahjanto, R.T., Prananto, Y.P., 2023. Leaching Optimization of Manganese Ore From North Central Timor Using H_2O_2 as A Reducing Agent. Indones. Min. J. 26, 19–27. https://doi.org/10.30556/imj.Vol26.No1.2023.1301

Anderson, J.., Peterson, R.., Swainson, I., 2012. The Atomic

Structure of Deuterated Boyleite $ZnSO_4 \cdot 4D_2O$, Ilesite $MnSO_4 \cdot 4D_2O$, and Bianchite $ZnSO_4 \cdot 6D_2O$. Am. Mineral. 97, 1905–1914.

Asghar, A., Iqbal, N., Noor, T., 2020. Comparison of BDC Linker Based MOFs for Carbon Dioxide Trapping; Curb Climate Change. IEEE Green Technol. Conf. 2020-April, 203–205. https://doi.org/10.1109/GreenTech46478.2020.9289756

Asghar, A., Iqbal, N., Noor, T., Kariuki, B.M., Kidwell, L., Easun, T.L., 2021. Efficient Electrochemical Synthesis of a Manganese-Based Metal-Organic Framework for H_2 and CO_2 Uptake. Green Chem. 23, 1220–1227. https://doi.org/10.1039/d0gc03292a

Bakri, H., Jafar, N., Jumadra, J., Yusuf, F.N., Firdaus, F., 2024. Characteristics of Host Rocks Manganese of The Anabanua Village Barru District South Sulawesi Province , Indonesia. J. Geosci. Eng. Environ. Technol. 9, 351–356. https://doi.org/10.25299/jgeet.2024.9.3.12833

Behera, J.N., Bhattacharjee, J., Horike, S., Marri, S.R., Dahiya, P.P., 2014. Synthesis and Characterization of Robust Three-Dimensional Chiral Metal Sulfates. RSC Adv. 4, 50435–50442. https://doi.org/10.1039/c4ra09471a

Caminiti, R., Marongiu, G., Paschina, G., 1982. A Comparative X-Ray Diffraction Study of Aqueos $MnSO_4$ an Crystals of $MnSO_4 \cdot 5H_2O$ Locality:Synthetic. Zeitschrift fur Naturforsch. A 37, 581–586.

Chakraborty, D., Bej, S., Chatterjee, R., Banerjee, P., Bhaumik, A., 2022. A New Phosphonate Based Mn-MOF in Recognising Arginine Over Lysine in Aqueous Medium and Other Bio-Fluids with "Sepsis" Disease Remediation. Chem. Eng. J. 446, 136916. https://doi.org/10.1016/j.cej.2022.136916

Chakraborty, I., Majumder, D., Rakshit, R., Alam, M., Mukherjee, S., Gorai, A., Mandal, K., 2021. Magnetic Field-Dependent Photoluminescence of Tartrate-Functionalized Gadolinium-Doped Manganese Ferrite Nanoparticles: A Potential Therapeutic Agent for Hyperbilirubinemia Treatment. ACS Appl. Nano Mater. 4, 4379–4387. https://doi.org/10.1021/acsanm.0c03073

Chen, J., Bai, B., Lei, J., Wang, P., Wang, S., Li, J., 2022. Mn_3O_4 Derived from Mn-MOFs with Hydroxyl Group Ligands for Efficient Toluene Catalytic Oxidation. Chem. Eng. Sci. 263, 118065. https://doi.org/10.1016/j.ces.2022.118065

Czaja, A.U., Trukhan, N., Müller, U., 2009. Industrial applications of metal–organic frameworks. Chem. Soc. Rev. 38, 1284–1293. https://doi.org/10.1039/b804680h

Dawadi, S., Gupta, A., Khatri, M., Budhathoki, B., Lamichhane, G., Parajuli, N., 2020. Manganese Dioxide Nanoparticles: Synthesis, Application and Challenges. Bull. Mater. Sci. 43, 1–10. https://doi.org/10.1007/s12034-020-02247-8

Dawood, S., Dorris, A., Davis, K., Hammer, N.I., Rathnayake, H., 2021. Synthesis, Characterization, and Photophysics of Self-Assembled Mn(II)-MOF with Naphthalene Chromophore. J. Phys. Chem. C 125, 792–802. https://doi.org/10.1021/acs.jpcc.0c09600

Dolomanov, O.V., Bourhis, L.J., Gildea, R.J., Howard, J.A.K., Puschmann, H., 2009. OLEX2: A Complete Structure Solution, Refinement and Analysis Program. J. Appl. Crystallogr. 339–341. https://doi.org/https://doi.org/10.1107/S0021889808042726

Elazar, M., Ph, D., 2022. Optimization of Metal Organic Framework (MOF) Synthesis for Use in Drug Delivery. Technium 4, 53–61.

Gandhimathi, R., Krishnan, C.M., Selvarajan, P., 2015. Growth and Characterization of Manganese Sulpho Tartrate (MST) - A Semiorganic NLO crystal. Optik (Stuttg). 126, 2925–2929. https://doi.org/10.1016/j.ijleo.2015.07.052

Ge, C., Zhao, Z., Han, G., Zhang, X., 2008. Poly[[diaqua-μ_4-tartrato-μ_2-tartrato- dimanganese(II)] dihydrate]. Acta Crystallogr. Sect. E Struct. Reports Online 64. https://doi.org/10.1107/S1600536807067839

Guo, X., Xiao, H.S., Wang, F., Zhang, Y.H., 2010. Micro-Raman and FTIR Spectroscopic Observation on The Phase Transitions of $MnSO_4$ Droplets and Ionic Interactions Between Mn^{2+} and SO_4^{2-}. J. Phys. Chem. A 114, 6480–6486. https://doi.org/10.1021/jp9104147

Hou, S., Zhang, H., Wang, P., Zhang, M., Yang, P., 2022. Multiwall Carbon Nanotube Decorated Hemin/Mn-MOF Towards BPA Degradation Through PMS Activation. J. Environ. Chem. Eng. 10, 108426. https://doi.org/10.1016/j.jece.2022.108426

Hu, H., Lou, X., Li, C., Hu, X., Li, T., Chen, Q., Shen, M., Hu, B., 2016. A Thermally Activated Manganese 1,4-benzenedicarboxylate Metal Organic Framework with High Anodic Capability for Li-Ion Batteries. New J. Chem. 40, 9746–9752. https://doi.org/10.1039/c6nj02179d

Insta Nano, 2025. XRD Crystallite (grain) Size Calculator (Scherrer Equation)-InstaNano. https://instanano.com/all/characterization/xrd/crystallite-size/ (accessed May 7th, 2025)

Jagtap, U.S., Patil, A.K., Talele, H.R., 2022. The Study of Manganese Metal Tartrate Crystals Grown by Agar-agar Gel Technique. Int. J. Basic Appl. Sci. 11, 91–95. https://doi.org/10.13140/RG.2.2.12036.81285

Jethva, H., Joshi, M., 2014. FTIR and Thermal Studies of Gel Grown Lead Cobalt Mixed Levo Tartrate Crystals. Int. J. Innov. Res. Sci. Eng. Technol. 03, 16517–16526. https://doi.org/10.15680/ijirset.2014.0310016

Jia, Y., ALOthman, Z.A., Liang, R., Cha, S., Li, X., Ouyang, W., Zheng, A., Osman, S.M., Luque, R., Sun, Y., 2020. Immobilization of (Tartrate-Salen)Mn(III) Polymer Complexes into SBA-15 for Catalytic Asymmetric Epoxidation of Alkenes. Mol. Catal. 495, 111146. https://doi.org/10.1016/j.mcat.2020.111146

Kaduk, J.A., 2002. Terephthalate Salts of Dipositive Cations. Acta Crystallogr. Sect. B 58, 815–822. https://doi.org/10.1107/S0108768102009102

Khunur, M.M., Prananto, Y.P., 2018. Coordination Polymers of M (II) Tartrate Hydrate (M= Cu, Mn, Cd) Crystallised from Aqueous Solution, in: Proceeding Book 8th Annual Basic Science International Conference - Indonesia. pp. 267–271.

Kusumaningrum, R., Abi, F.D.Y.P., Sukmarani, G., Habieb, A.M., Fauzi, F., Widayatno, W.B., Wismogroho, A.S., Amal, M.I., Rochman, N.T., Noviyanto, A., 2020. Shape Modification of Manganese Oxide Prepared by Solvothermal: Effect of Precipitation Agent. IOP Conf. Ser. Mater. Sci. Eng. 924, 12013. https://doi.org/10.1088/1757-899X/924/1/012013

Kusumaningrum, R., Rahmani, S.A., Widayatno, W.B., Wismogroho, A.S., Nugroho, D.W., Maulana, S., Rochman, N.T., Amal, M.I., 2018. Characterization of Sumbawa Manganese Ore and Recovery of

Manganese Sulfate as Leaching Products. AIP Conf. Proc. 1964, 20042. https://doi.org/10.1063/1.5038324

Lee, Y.R., Kim, J., Ahn, W.S., 2013. Synthesis of Metal-Organic Frameworks: A Mini Review. Korean J. Chem. Eng. 30, 1667–1680. https://doi.org/10.1007/s11814-013-0140-6

Li, B.G., Mi, J., Nie, F.M., 2010. Solid-State Synthesis and Structural Characterization of Hydrated Zinc (II) Tartrate Complex. J. Chem. Crystallogr. 40, 29–33. https://doi.org/10.1007/s10870-009-9600-6

Li, Q., Rao, X., Xu, B., Yang, Y., Liu, T., Jiang, T., Hu, L., 2017. Extraction of Manganese and Zinc from Their Compound Ore by Reductive Acid Leaching. Trans. Nonferrous Met. Soc. China 27, 1172–1179. https://doi.org/https://doi.org/10.1016/S1003-6326(17)60137-7

Lide, D.R., 2010. CRC Handbook of Chemistry and Physics, 90th Edition (CD-ROM Version 2010), 90th ed. Taylor \& Francis.

Ma, D., Huang, X., Zhang, Y., Wang, L., Wang, B., 2023. Metal-Organic Frameworks: Synthetic Methods for Industrial Production. Nano Res. 16, 7906–7925.

Nakamoto, K., 2006. Infrared and Raman Spectra of Inorganic and Coordination Compounds, in: Handbook of Vibrational Spectroscopy. John Wiley & Sons, Ltd. https://doi.org/https://doi.org/10.1002/0470027320.s4104

Nyquist, R.A., Kagel, R.O., 1971. Infrared Spectra of Inorganic Compounds. Handb. Infrared Raman Spectra Inorg. Compd. Org. Salts 1–18. https://doi.org/10.1016/b978-0-12-523450-4.50005-5

OChemOnline, 2011. Infrared Spectroscopy Absorption Table - OChemOnline [WWW Document]. LibreTexts. URL https://chem.libretexts.org/Bookshelves/Ancillary_Materials/Reference/Reference_Tables/Spectroscopic_Parameters/Infrared_Spectroscopy_Absorption_Table#

Paulose, R., Mohan, R., 2019. Hausmannite (Mn_3O_4) - Synthesis and Its Electrochemical, Catalytic and Sensor Application. Photoenergy Thin Film Mater. 283–320. https://doi.org/10.1002/9781119580546.ch7

Prananto, Y.P., Wibisono, R.D., Fadhilah, S.G., Tjahjanto, R., Darjito, Salsabila, F.L., 2022. Crystallization of Mn(II) and Cd(II) Complexes in A Water-Methanol System: Tartrate vs Nicotinamide Ligand Selectivity. Acta Chim. Asiana 5, 166–172. https://doi.org/10.29303/aca.v5i1.114

Sagar, R., Rao, A., Prathap, C., 2021. Growth, Characterization and SHG Studies of Cu (II) Doped Manganese Sulfate Monohydrate Crystals. Opt. Quantum Electron. 53, 1–10. https://doi.org/10.1007/s11082-021-03177-3

Sagunthala, P., Yasotha, P., Vijaya, L., 2013. Growth and Characterization of Manganese (II) Sulphate and L-Lysine Doped Manganese (II) Sulphate ($LMnSO_4$) Crystals. Int. J. Sci. Eng. Appl. 7560, 46–52. https://doi.org/10.7753/ijseancrtam.1012

Sandag-Ochir, S., Tsedendamba, Z., Batkhuyag, O., Lkhasuren, J., Dashkhuu, K., Namsrai, S.-E., Dashtseren, B., Buyannasan, U., Enkhtur, O., 2021. Beneficiation and Sulfuric Acid Leaching of Manganese Ore. Proc. 5th Int. Conf. Chem. Investig. Util. Nat. Resour. 2, 158–163. https://doi.org/10.2991/ahcps.k.211004.022

Santos, P.F., Luz, P.P., 2020. Synthesis of a CE-based MOF-76 with High Yield: A Study of Reaction Parameters based on a Factorial Design. J. Braz. Chem. Soc. 31, 566–573. https://doi.org/10.21577/0103-5053.20190218

Saravanabharathi, D., Murugavel, S.C., 2021. Rapid Crystallization Strategy for Manganese(II) - L - Tartrate. EAI. https://doi.org/10.4108/eai.7-12-2021.2314727

Stock, N., Biswas, S., 2012. Synthesis of Metal-Organic Frameworks (MOFs): Routes to Various MOF Topologies, Morphologies, and Composites. Chem. Rev. 112, 933–969. https://doi.org/https://doi.org/10.1021/cr200304e

Sumardi, S., Mubarok, M.Z., Saleh, N., 2013. Pengolahan Bijih Mangan Menjadi Mangan Sulfat Melalui Pelindian Reduktif Menggunakan Asam Oksalat Dalam Suasana Asam. Semirata FMIPA Univ. Lampung 123–130.

Sundriyal, S., Mishra, S., Deep, A., 2019a. Study of Manganese-1,4-benzenedicarboxylate Metal Organic Framework Electrodes Based Solid State Symmetrical Supercapacitor. Energy Procedia 158, 5817–5824. https://doi.org/10.1016/j.egypro.2019.01.546

Sundriyal, S., Shrivastav, V., Sharma, M., Mishra, S., Deep, A., 2019b. Redox Additive Electrolyte Study of Mn–MOF Electrode for Supercapacitor Applications. ChemistrySelect 4, 2585–2592. https://doi.org/10.1002/slct.201900305

Supriadi, A., Sunarti, Kencono, A.W., Kurniasih, T.N., Prasetyo, B.E., Kurniawan, F., Kurniadi, C.B., Alwendra, Y., Aprilia, R., Rabbani, Q., Setiadi, I., Anggraeni, D., 2017. Kajian Dampak Hilirisasi Mineral Mangan Terhadap Perekonomian Regional. Pusat Data dan Teknologi Informasi Energi dan Sumber Daya Mineral Kementrian Energi dan Sumber Daya Mineral, Jakarta.

Yadav, S., Sharma, S., Dutta, S., Sharma, A., Adholeya, A., Sharma, R.K., 2020. Harnessing the Untapped Catalytic Potential of A $CoFe_2O_4$/Mn-BDC Hybrid MOF Composite for Obtaining A Multitude of 1,4-Disubstituted 1,2,3-Triazole Scaffolds. Inorg. Chem. 59, 8334–8344. https://doi.org/10.1021/acs.inorgchem.0c00752

Yang, Y., Qi, X.X., Chen, H.R., Wang, X.Y., Yang, X.L., Tu, Y.Y., Zhou, T., Jiang, T., Wang, F., Chen, Z., Ju, Y.C., 2020. Synthesis, Crystal Structures and Luminescent Properties of Zn(II)/Cd(II) Metal–Organic Frameworks Constructed by 1,4-Benzenedicarboxylic Acid and 4,4′-(2,5-Difluoro-1,4-phenylene)dipyridine. J. Inorg. Organomet. Polym. Mater. 30, 4289–4296. https://doi.org/10.1007/s10904-020-01627-1

Yusuf, N.J., Arifin, Y.I., Hutagalung, R., Manyoe, I.N., 2023. Study of Boalemo Red Limestone for Geotourism Development based on Lithological, Geochemical Analysis and Geological Heritage Assessment. J. Geosci. Eng. Environ. Technol. 8, 212–220. https://doi.org/10.25299/jgeet.2023.8.3.12075

Zhang, X., Zhao, Z., Zhao, S., Xiang, S., Gao, W., Wang, L., Xu, J., Wang, Y., 2022. The Promoting Effect of Alkali Metal and H_2O on Mn-MOF Derivatives for Toluene Oxidation: A Combined Experimental and Theoretical Investigation. J. Catal. 415, 218–235.

https://doi.org/10.1016/j.jcat.2022.10.005
Zhao, T., Zhu, H., Geng, W., Zou, M., Dong, M., Ying, J., 2022. Morphology Control Synthesis of Cr-Benzenedicarboxylate MOFs for The Removal of Methylene Blue. J. Solid State Chem. 305, 122651. https://doi.org/10.1016/j.jssc.2021.122651
Zheng, Z., Alawadhi, A.H., Yaghi, O.M., 2023. Green Synthesis and Scale-Up of MOFs for Water Harvesting from Air. Mol. Front. J. 7, 1–20. https://doi.org/10.1142/s2529732523400011